

PROCEEDINGS OF SPIE

***Photonics Applications in
Astronomy, Communications,
Industry, and High Energy
Physics Experiments 2021***

**Ryszard S. Romaniuk
Andrzej Smolarz
Waldemar Wojcik**
Editors

**31 May – 1 June 2021
Warsaw, Poland**

Sponsored and Published by
SPIE

Volume 12040

Proceedings of SPIE 0277-786X, V. 12040

SPIE is an international society advancing an interdisciplinary approach to the science and application of light.

Photonics Applications in Astronomy, Communications, Industry, and High Energy Physics Experiments 2021
edited by Ryszard S. Romaniuk, Andrzej Smolarz, Waldemar Wojcik, Proc. of SPIE
Vol. 12040, 1204001 · © 2021 SPIE · 0277-786X · doi: 10.1117/12.2620356

Proc. of SPIE Vol. 12040 1204001-1

The papers in this volume were part of the technical conference cited on the cover and title page. Papers were selected and subject to review by the editors and conference program committee. Some conference presentations may not be available for publication. Additional papers and presentation recordings may be available online in the SPIE Digital Library at SPIDigitalLibrary.org.

The papers reflect the work and thoughts of the authors and are published herein as submitted. The publisher is not responsible for the validity of the information or for any outcomes resulting from reliance thereon.

Please use the following format to cite material from these proceedings:

Author(s), "Title of Paper," in *Photonics Applications in Astronomy, Communications, Industry, and High Energy Physics Experiments 2021*, edited by Ryszard S. Romaniuk, Andrzej Smolarz, Waldemar Wojcik, Proc. of SPIE 12040, Seven-digit Article CID Number (DD/MM/YYYY); (DOI URL).

ISSN: 0277-786X
ISSN: 1996-756X (electronic)

ISBN: 9781510649552
ISBN: 9781510649569 (electronic)

Published by

SPIE

P.O. Box 10, Bellingham, Washington 98227-0010 USA

Telephone +1 360 676 3290 (Pacific Time)

SPIE.org

Copyright © 2021 Society of Photo-Optical Instrumentation Engineers (SPIE).

Copying of material in this book for internal or personal use, or for the internal or personal use of specific clients, beyond the fair use provisions granted by the U.S. Copyright Law is authorized by SPIE subject to payment of fees. To obtain permission to use and share articles in this volume, visit Copyright Clearance Center at copyright.com. Other copying for republication, resale, advertising or promotion, or any form of systematic or multiple reproduction of any material in this book is prohibited except with permission in writing from the publisher.

Printed in the United States of America by Curran Associates, Inc., under license from SPIE.

Publication of record for individual papers is online in the SPIE Digital Library.

SPIE. DIGITAL LIBRARY

SPIDigitalLibrary.org

Paper Numbering: A unique citation identifier (CID) number is assigned to each article in the Proceedings of SPIE at the time of publication. Utilization of CIDs allows articles to be fully citable as soon as they are published online, and connects the same identifier to all online and print versions of the publication. SPIE uses a seven-digit CID article numbering system structured as follows:

- The first five digits correspond to the SPIE volume number.
- The last two digits indicate publication order within the volume using a Base 36 numbering system employing both numerals and letters. These two-number sets start with 00, 01, 02, 03, 04, 05, 06, 07, 08, 09, 0A, 0B ... 0Z, followed by 10-1Z, 20-2Z, etc. The CID Number appears on each page of the manuscript.

12040 OG **Differential Mueller-matrix tomography of the polycrystalline structure of biological tissues with different damage durations** [12040-36]

PHOTONIC SENSORS, DEVICES, AND SYSTEMS

12040 OH **Development of the IR camera with the Micro80Gen2™ microbolometric detector** [12040-5]

12040 OI **Optoimmittance converters** [12040-11]

12040 OJ **Weather sensing device with local sensors and application of IoT methods** [12040-12]

12040 OK **Concept of chemical subsystem of the innovative system for detecting hidden people in transport (CHS-ISDHPT) (Invited Paper)** [12040-13]

12040 OL **An interferometer with continuously variable bandpass filter (Invited Paper)** [12040-14]

12040 OM **Topology changes of MESH network used in mobile distribution point of ICT infrastructure** [12040-15]

12040 ON **Analysis of the development approaches of the system of audio synthesis and recognition with the option of using photonic processors** [12040-16]

12040 OO **New directions in the construction of tokamak plasma impurity diagnostics systems** [12040-17]

12040 OP **Comparison of implementation methods for data processing algorithms on FPGA** [12040-18]

12040 OQ **Object-oriented hardware-software model based on novel CII concept** [12040-25]

12040 OR **RF front-end for long distance WiFi communication** [12040-26]

12040 OS **Laser illumination in triangulation vision systems (Invited Paper)** [12040-27]

12040 OT **Quality control automation of metallic surface using machine vision** [12040-28]

12040 OU **Spaceborne SAR ship-detection system using FPGA SoCs with integrated ADCs/DACs** [12040-30]

12040 OV **Computer-integrated technology of space television cameras radiometric calibration (Invited Paper)** [12040-38]

12040 OW **The influence of the TFBG tilt angle on the spectral response** [12040-39]

12040 OX **A continuous, non-interferent linac electron beam energy measurement system for radiation processing installation** [12040-40]

PROCEEDINGS OF SPIE

[SPIDigitalLibrary.org/conference-proceedings-of-spie](https://spiedigitallibrary.org/conference-proceedings-of-spie)

Differential Mueller-matrix tomography of the polycrystalline structure of biological tissues with different damage durations

Anatoly Stashkevich, Oleh Ya. Wanchulyak, Olexandra Yu. Litvinenko, Yuriy Ushenko, Olexander Dubolazov, et al.

Anatoly T. Stashkevich, Oleh Ya. Wanchulyak, Olexandra Yu. Litvinenko, Yuriy O. Ushenko, Olexander V. Dubolazov, Elena Sorochan, Lubov V. Zagoruiko, Waldemar Wójcik, Saule Rakhmetullina, Nataliya Denissova, Daniyar Jarykbassov, "Differential Mueller-matrix tomography of the polycrystalline structure of biological tissues with different damage durations," Proc. SPIE 12040, Photonics Applications in Astronomy, Communications, Industry, and High Energy Physics Experiments 2021, 120400G (3 November 2021); doi: 10.1117/12.2617360

SPIE.

Event: Photonics Applications in Astronomy, Communications, Industry, and High Energy Physics Experiments 2021 (WILGA 2021), 2021, Warsaw, Poland

Differential Mueller-matrix tomography of the polycrystalline structure of biological tissues with different damage durations

Anatoly T. Stashkevich^{*a}, Oleh Ya. Wanchulyak^b, Olexandra Yu. Litvinenko^b, Yuriy O. Ushenko^c,
Olexander V. Dubolazov^c, Elena M. Sorochan^d, Lubov V. Zagoruiko^c, Waldemar Wojcik^f,
Saule Rakhmetullina^g, Nataliya Denissova^g, Daniyar Jarykbassov^h

^aSI The Institute of Traumatology and Orthopedics by NAMS of Ukraine, Kyiv, Ukraine;

^bBukovinian State Medical University, Teatral'na Square, 2, 58000 Chernivtsi, Ukraine; ^cChernivtsi National University, Kotsyubyns'koho St, 2, 58012 Chernivtsi, Ukraine; ^dPryazovskyi State Technical University Department of Biomedical Engineering, Universytets'ka Street, 7, 87500 Mariupol', Ukraine; ^eStus National University of Donetsk, 600-Richchya St, 21, 21000 Vinnytsia, Ukraine; ^fLublin University of Technology, Nadbystrzycka 38A, 20-618 Lublin, Poland; ^gEast Kazakhstan State Technical University named after D.Serikbayev, Ust-Kamenogorsk, Kazakhstan; ^hAcademy of Logistics and Transport, Almaty, Kazakhstan;

ABSTRACT

The work is aimed at the development and experimental testing of the polarization method for analyzing the polycrystalline structure of the human biological tissues. The main relationships between temporary changes in the statistical structure of topographic maps of the degree of crystallization of histological sections of the internal organs of a person and variations in the magnitude of the statistical moments of the 1st - 4th orders that characterize them are revealed. It is shown that with an increase in the damage duration, the statistical parameters of linear birefringence maps change according to the following scenario — the average and dispersion values decrease, asymmetry and excess, on the contrary, increase.

Keywords: polarimetry; laser image; diagnostics; histological sections of the internal organs

1. INTRODUCTION

Determining the prescription of death, improving the accuracy of its installation in the first hours, as well as determining its cause is one of the most important problems of forensic medicine¹. Known methods for determining the onset of the time of death are approximate and based on assessing the rate of onset of degenerative-dystrophic changes in soft tissues².

One of the ways to improve the sensitivity of these techniques is the application of the formalism of polarization, coherent, fractal and singular optics^{3,4}.

The aim of the study is to develop new forensic criteria for expanding the functionality and improving the accuracy of establishing the duration of damage to human internal organs according to the data of a multivariable digital histological study of brain, liver, and kidney tissues.

To achieve this goal, the following tasks were solved:

1. Development, substantiation and experimental testing of a complex of a new tomographic method for digital histological forensic medical research of temporary changes in polycrystalline and molecular optically anisotropic structure of tissues of internal organs with different age of damage.
2. To assess the diagnostic capabilities of the statistical analysis of the data of tomographic methods for examining samples of the brain, liver and kidney of a corpse in the forensic histological determination of the duration of damage to internal organs^{5,6,7}.
3. To investigate the relationship of temporal changes in the magnitude of statistical moments of the 1st - 4th orders, characterizing the distribution of the magnitude of the parameters of the tomographic method and the duration of damage.

*stashkat@i.ua; phone +38(044)486-32-03; ito.gov.ua

2. DIFFERENTIAL DECOMPOSITION OF THE MUELLER MATRIX OF BIOLOGICAL LAYERS

To describe the processes of transformation of the polarization structure of optical radiation by partial optically anisotropic layers, the following algorithm was obtained⁵ in terms of the parameters of the Stokes vector $S = \{S_1; S_2; S_3; S_4\}$.

$$\frac{dS}{dr} = \{M\}(r)S(r), \quad (1)$$

where $\{M\}(r)$ - Mueller differential matrix; $S(r)$ - Stokes vector of optical radiation at a distance r in a medium.

To represent the optical properties of an anisotropic medium using the formalism of the Mueller matrix, expression (1) takes the following form^{6,8,9}:

$$\frac{d\{F\}(r)}{dr} = \{F\}(r)\{M\}(r), \quad (2)$$

where $\{F\}(r)$ - Mueller matrix of a phase-inhomogeneous object in the plane of the partial layer located at a distance r . For single scattering (non-depolarizing) layers, the symmetry of the differential matrix $\{M\}(r)$ is a combination of six polarization properties:

$$\{M\} = \begin{bmatrix} 0 & m_{12} & m_{13} & m_{14} \\ m_{21} & 0 & m_{23} & -m_{24} \\ m_{31} & -m_{32} & 0 & m_{34} \\ m_{41} & m_{42} & -m_{43} & 0 \end{bmatrix} = \begin{bmatrix} 0 & LD_{0,90} & LD_{45,135} & CD \\ LD_{0,90} & 0 & CB & -LB_{45,135} \\ LD_{45,135} & -CB & 0 & LB_{0,90} \\ CD & LB_{45,135} & -LB_{0,90} & 0 \end{bmatrix}, \quad (3)$$

where: $LD_{0,90}$ and $LB_{0,90}$ - linear dichroism and birefringence for the direction of the optical axis $\rho = 0^\circ$; $LD_{45,135}$ and $LB_{45,135}$ - linear dichroism and birefringence for the direction of the optical axis $\rho = 45^\circ$; CD and CB - circular dichroism and birefringence.

In what follows, we will use the generalized linear birefringence parameters to analyze the optical anisotropy of the polycrystalline structure of biological layers (LB):

$$LB = \sqrt{LB_{0,90}^2 + LB_{45,135}^2}. \quad (4)$$

3. DIGITAL HISTOLOGICAL DIAGNOSIS OF PRESCRIPTION OF LIVER DAMAGE BY LINEAR BIREFRINGENCE TOMOGRAPHY

Fragments of Fig. 1 illustrates the results of a digital tomographic histological study of the degree of crystallization of liver tissue samples^{10,11,12}. Comparison of the coordinate and topographic structure of the maps of linear birefringence of histological sections of the liver showed¹²⁻¹⁷:

- significant variation in the degree of crystallization of liver samples;
- monotonous smoothing of fluctuations of linear birefringence with an increase in damage duration - 6 hours. (Fig. 1, fragment (2)) and 18 hours (Fig. 1, fragment (3)).

Analysis of statistical monitoring data on changes in coordinate distributions of the degree of crystallization of the substance of liver samples showed diagnostic capabilities similar to brain samples of digital tomographic histological examination of the prescription of damage - an increase in the duration and increase in the intervals of linear change, - table 1.

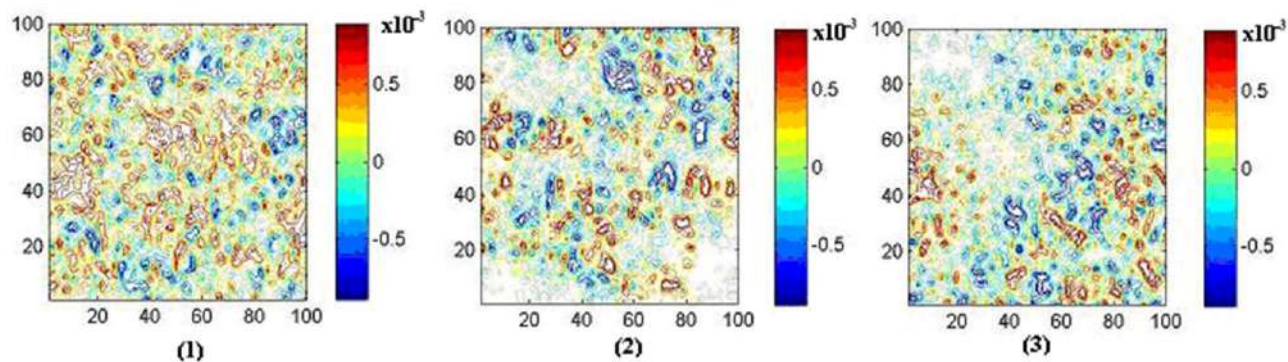


Figure 1. Maps of linear birefringence ($\times 4$) of histological sections of the liver of the dead from the control (1), research groups (6 hours - (2)) and (18 hours - (3)).

Table 1. Temporal dynamics of changes in statistical moments of the 1st - 4th orders characterizing the distribution of the magnitude of the linear birefringence ($4X$) of histological sections of the liver.

T, h.	2	4	6	12	18
$SM_1 \times 10^{-3}$	0.49 ± 0.021	0.38 ± 0.018	0.27 ± 0.012	0.16 ± 0.007	0.13 ± 0.08
p	$p \leq 0.05$			$p \leq 0.05$	
$SM_2 \times 10^{-3}$	0.29 ± 0.013	0.21 ± 0.008	0.13 ± 0.006	0.11 ± 0.04	0.12 ± 0.05
p	$p \leq 0.05$			$p \leq 0.05$	
SM_3	1.37 ± 0.055	1.45 ± 0.067	1.64 ± 0.071	2.03 ± 0.092	2.35 ± 0.11
p	$p \leq 0.05$			$p \leq 0.05$	
SM_4	1.76 ± 0.071	2.01 ± 0.098	2.25 ± 0.11	2.75 ± 0.13	3.21 ± 0.15
p	$p \leq 0.05$			$p \leq 0.05$	
T, h.	24	48	72	96	120
$SM_1 \times 10^{-3}$	0.12 ± 0.009	0.14 ± 0.008	0.12 ± 0.007	0.13 ± 0.008	0.12 ± 0.007
p	$p \leq 0.05$			$p \leq 0.05$	
$SM_2 \times 10^{-3}$	0.13 ± 0.009	0.11 ± 0.007	0.14 ± 0.008	0.14 ± 0.008	0.13 ± 0.007
p	$p \leq 0.05$			$p \leq 0.05$	
SM_3	2.73 ± 0.12	3.05 ± 0.14	3.11 ± 0.15	3.12 ± 0.16	3.18 ± 0.14
p	$p \leq 0.05$			$p \leq 0.05$	
SM_4	3.72 ± 0.16	4.18 ± 0.19	4.31 ± 0.21	4.49 ± 0.21	4.64 ± 0.22
p	$p \leq 0.05$			$p \leq 0.05$	

The following characteristics of the duration and number of time intervals of linear and statistically significant (0.05) changes in the eigenvalues of the set of statistical moments of the 1st - 4th orders were experimentally determined:

- the average within the representative groups of liver samples of linear birefringence distributions up to 12 hours with a dynamic range of 0.33;
- dispersion of the scatter of random values of the degree of crystallization within representative groups of liver samples up to 12 hours with a dynamic range of 0.16.
- asymmetries in the distributions of linear birefringence within the representative groups of liver samples — the diagnostic interval lasts up to 48 hours from two linear sections 1 hour - 24 hours and 24 hours - 48 hours with a dynamic range of 1.68;
- excess — linear birefringence distributions within representative groups of liver samples — diagnostic interval up to 48 hours. of the two linear sections 1 hour - 24 hours and 24 hours - 48 hours with a dynamic range of 1.98.

The results of polarization tomography of digital histological studies of large-scale (40x) topographic maps of linear birefringence of histological sections of the liver are shown in fig. 2.

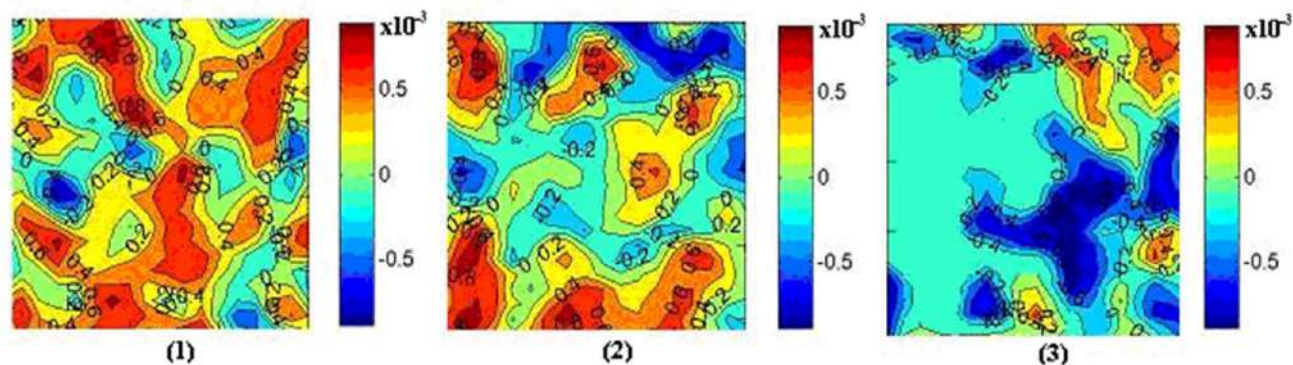


Figure 2. Maps of the distributions of linear birefringence ($\times 40$) of histological sections of the liver of the deceased from the control group (1), research groups with different damage durations (6 hours - (2)) and (18 hours - (3)).

A statistical analysis of the temporal changes in the topographic distributions of the degree of crystallization is given in the data series of table 2. Tables 3 to 5 show time intervals and accuracy of the method for reconstructing the polycrystalline structure of histological sections of tissues.

Table 2. Temporal dynamics of changes in statistical moments of the 1st - 4th orders characterizing the distribution of the magnitude of the linear birefringence ($40X$) of histological sections of the liver.

<i>T, h.</i>	2	4	6	12	18
$SM_1 \times 10^{-3}$	0.48 ± 0.014	0.43 ± 0.011	0.38 ± 0.009	0.28 ± 0.007	0.18 ± 0.005
$SM_2 \times 10^{-3}$	0.29 ± 0.009	0.23 ± 0.008	0.17 ± 0.006	0.11 ± 0.004	0.05 ± 0.002
SM_3	1.53 ± 0.055	1.74 ± 0.067	1.93 ± 0.071	2.21 ± 0.092	2.54 ± 0.11
SM_4	1.87 ± 0.071	2.08 ± 0.098	2.29 ± 0.11	2.78 ± 0.13	3.31 ± 0.15
<i>T, h.</i>	24	48	72	96	120
$SM_1 \times 10^{-3}$	0.08 ± 0.003	0.03 ± 0.001	0.02 ± 0.001	0.03 ± 0.002	0.02 ± 0.001
$SM_2 \times 10^{-3}$	0.02 ± 0.001	0.25 ± 0.001	0.23 ± 0.001	0.24 ± 0.0012	0.23 ± 0.0012
SM_3	2.92 ± 0.13	3.29 ± 0.15	3.67 ± 0.16	3.35 ± 0.15	3.42 ± 0.12
SM_4	3.73 ± 0.17	4.16 ± 0.18	4.87 ± 0.21	4.63 ± 0.21	4.79 ± 0.21

Table 3. Time intervals and accuracy of the method for reconstructing the polycrystalline structure of brain tissue sections.

Statistical moments	Interval, h		Accuracy, min.	
	4x	40x	4x	40x
Increase	1-24	1-24	45	35
Average	24-48	24-72	55	45
Dispersion	1-24	1-24	45	35
Asymmetry	24-48	24-72	55	45
Excess	1-24	1-24	35	25
	24-72	24-120	50	45

Table 4. Time intervals and accuracy of the method for reconstructing the polycrystalline structure of liver tissue sections.

Statistical moments	Interval, h		Accuracy, min.	
	4x	40x	4x	40x
Increase	1-24	1-24	45	35
Average	24-48	24-72	55	45
Dispersion	1-24	1-24	45	35
Asymmetry	24-48	24-72	55	45
Excess	1-24	1-24	35	25
	24-72	24-120	50	45

Table 5. Time intervals and accuracy of the method for reconstructing the polycrystalline structure of kidney tissue sections.

Increase	4x	40x	4x	40x
Average	1-24	1-24	45	35
	24-48	24-72	55	45
Dispersion	1-24	1-24	45	35
	24-48	24-72	55	45
Asymmetry	1-24	1-24	35	25
	24-72	24-120	50	45
Excess	1-24	1-24	35	25
	24-72	24-120	50	45

An analysis of the results of a large-scale polarization reconstruction of the degree of crystallization of liver samples revealed similar patterns (but with a different range of eigenvalues) to digital tomographic histology of brain samples — an increase (from 2 to 8 times) in the time duration for determining the age of liver tissue damage based on detection linear intervals of change in the magnitude of statistical moments of the 1st - 4th orders (average, dispersion, asymmetry and excess), which characterize the topographic linear birefringence maps of representative choosing samples from the control and research groups^{18,19}:

- the average distribution of the degree of crystallization is two linear intervals of 1 hour – 24 hours. and 24 hours - 48 hours and a range of variation of the eigenvalues of 0.045;
- dispersion of the distribution of the degree of crystallization – a linear interval of 24 hours and a range of variation of the eigenvalues of 0.27;
- asymmetry of the distribution of the degree of crystallization – two linear intervals of 1 hour - 24 hours. and 24 hours - 72 hours and a range of variation of the eigenvalues of 2.14;
- excess of the distribution of the degree of crystallization – two linear intervals of 1 hour – 24 hours and 24 hours – 72 hours and a range of variation of the eigenvalues of 2.99

CONCLUSION

By applying the method of digital histological research to the original algorithmic reproduction of maps of the degree of crystallization of the substance of tissues of the internal organs of a person with different damage durations, changes in the morphological and biochemical structures of the tissues of the brain, liver and kidney were studied for the first time over a time interval from 1 hour to 120 hours.

For the first time, the main relationships between temporary changes in the statistical structure of topographic maps of the degree of crystallization of histological sections of the internal organs of a person and variations in the magnitude of the statistical moments of the 1st - 4th orders that characterize them are revealed.

It is shown that with an increase in the damage duration, the statistical parameters of linear birefringence maps change according to the following scenario — the average and dispersion values decrease, asymmetry and excess, on the contrary, increase.

The time ranges of linear change in the variation of the magnitude of the statistical indicators of the tomographic method of digital histology and the accuracy of determining the prescription of damage are established.

Small-scale crystallization maps (4x):

- average – 48 hours, accuracy 45 minutes – 55 minutes;
- dispersion – 48 hours, accuracy 45 minutes – 55 minutes;
- asymmetry – 72 hours, accuracy 35 minutes – 50 minutes;
- excess – 72 hours, accuracy 35 minutes – 50 minutes

Large-scale crystallization maps (40x):

- average – 72 hours, accuracy 35 minutes – 45 minutes;
- dispersion – 72 hours, accuracy 35 minutes – 45 minutes;
- asymmetry – 120 hours, accuracy 25 minutes – 45 minutes;
- excess – 120 hours, accuracy 25 minutes – 45 minutes.

ACKNOWLEDGMENT

This work was supported by the National Research Foundation of Ukraine, project No. 2020.02 / 0061

REFERENCES

- [1] Lu, S. and Chipman, A., "Interpretation of Mueller matrices based on polar decomposition," *J. Opt. Soc. Am. A.*, 13(1), 1106-1113 (1996).
- [2] Ghosh N. and Vitkin A., "Techniques for fast and sensitive measurements of two-dimensional birefringence distributions," *Journal of Biomedical Optics.*, 16(11), 110801 (2011).
- [3] Tuchin, L. W., and Zimnyakov, D. A., [Optical polarization in biomedical applications], New York, USA (2006).
- [4] Ushenko, A.G., Dubolazov, O.V., Bachynsky, V.T., Peresunko, A.P. and Vanchulyak, O.Y., "On the feasibilities of using the wavelet analysis of mueller matrix images of biological crystals," *Advances in Optical Technologies*, 162832 (2010).
- [5] Zabolotna, N.I., Wojcik, W., Pavlov, S.V., Ushenko, O.G., Suleimenov, B., "Diagnostics of pathologically changed birefringent networks by means of phase Mueller matrix tomography," *Proceedings of SPIE - The International Society for Optical Engineering*, 86980 (2013).
- [6] Ushenko, A.G., "Correlation processing and wavelet analysis of polarization images of biological tissues," *Optics and Spectroscopy (Optika i Spektroskopiya)*, 91 (5), 773-778 (2001).
- [7] Zabolotna, N.I., Wojcik, W., Pavlov, S.V., Ushenko, O.G. and Suleimenov, B., "Diagnostics of pathologically changed birefringent networks by means of phase Mueller matrix tomography," *Proceedings of SPIE - The International Society for Optical Engineering*, 86980 (2013).
- [8] Ushenko, A.G., "Correlation processing and wavelet analysis of polarization images of biological tissues," *Optics and Spectroscopy (Optika i Spektroskopiya)*, 91 (5), 773-778 (2001).
- [9] Isaieva, O. A., Avrunin, O. G., Moroz, I. I., Stoliarenko, O. V., Akselrod, R. B., Kylyvnyk, V. S. and Kozbakova, A., "Features of image analysis under UV-video dermoscopy," *Proceedings of SPIE - the International Society for Optical Engineering*, 11456 (2020). doi:10.1117/12.2569774
- [10] Kovalova, A., Shushliapina, N., Avrunin, O., Zlepko, A., Pugach, S., Burennikova, N. and Smailova, S., "Possibilities of automated image processing at optical capillaroscopy," *Proceedings of SPIE - the International Society for Optical Engineering*, 11456 (2020). doi:10.1117/12.2569772
- [11] Selivanova, K. G., Avrunin, O. G., Zlepko, S., Guminskyi, Y. Y., Poplavskyy, O. A. and Gromaszek, K., "The tracking system of a three-dimensional position of hand movement fortremor detection," *Proceedings of SPIE - the International Society for Optical Engineering*, 115810I (2020).
- [12] Wójcik, W. and Smolarz, A. and Pavlov, S. V., [Information technology in medical diagnostics], Taylor & Francis Group, CRC Press, Balkema book, London, 1-210 (2017).
- [13] Wójcik, W., Pavlov, S. and Kalimoldayev, M., [Information technology in medical diagnostics II], Taylor & Francis Group, CRC Press, Balkema book, London, 1-336 (2019).
- [14] Kozlovska, T. I. and Pavlov, S. V., [Optoelectronic means of diagnosing human pathologies associated with peripheral blood circulation], LAP LAMBERT Academic Publishing, Beau Bassin 71504, Mauritius, 1-56 (2019).
- [15] Omiotek, Z., Prokop, P., "The construction of the feature vector in the diagnosis of sarcoidosis based on the fractal analysis of CT chet images," *Informatyka, Automatyka, Pomiary W Gospodarce I Ochronie Środowiska*, 9(2), 16-23 (2019).
- [16] Korchenko, A., Tereykovcky, I., Aytkhozhaeva, E., Seilova, N., Kosyuk, Y., Wojcik, W., Komada, P. & Sikora, J., "Efficiency evaluating method for the devices with infrasound impact on the computer equipment functioning," *International Journal of Electronics and Telecommunications*, 64(2) (2018).
- [17] Tymkovich, M. Y., Avrunin, O. G., Paliy, V. G., et al., "Automated method for structural segmentation of nasal airways based on cone beam computed tomography," *Proc. SPIE* 10445, (2017).
- [18] Kolobrodov, V. G., Kolobrodov, M. S. and Tymchyk G. S. "The diffraction limit of an optical spectrum analyzer," *Proceedings of SPIE – The International Society for Optical Engineering*, 98090F, p.9809 (2015).
- [19] Kolobrodov V.G., Mykytenko V.I., Kolobrodov M.S., Tymchyk G.S. "Physical and mathematical model of the digital coherent optical spectrum analyzer," *Optica Applicata*, 47(2), 273-282 (2017).